Supporting Information

Abundance of Low-Energy Oxygen Vacancy Pairs Dictates the Catalytic Performance of Cerium-Stabilized Zirconia

Yao Peng [a], Xia-Lan Si [a], Cheng Shang[a,c,*], and Zhi-Pan Liu [a,b,c,*]

[a] *Shanghai Key Laboratory of Molecular Catalysis and Innovative Materials, Key Laboratory of Computational Physical Science, iChEM, Department of Chemistry, Fudan University, Shanghai 200433, China*
[b] *Key Laboratory of Synthetic and Self-Assembly Chemistry for Organic Functional Molecules, Shanghai Institute of Organic Chemistry, Chinese Academy of Sciences, Shanghai 200032, China*
[c] *Shanghai Qi Zhi Institution, Shanghai 200030, China*

1. The calculation detail of Bayesian guided active learning process

In brief, the G-NN potential is firstly generated by the standard SSW-NN process via the iterative self-learning of the plane wave density functional theory (DFT) global PES dataset generated from SSW exploration. There are three steps: (i) global dataset generation based on DFT calculations using selected structures from SSW simulation from random bulk structures, and bulk and slab structures collected from several previous works (ii) G-NN potential fitting and (iii) SSW global optimization using G-NN potential. These three steps are iteratively performed until the G-NN potential is transferable and robust enough to describe the global PES. Second, Bayesian optimization is utilized to drive the iterative acquisition-surrogate procedure, i.e. predicting the global minimum (GM) structures by SSW-NN searches and updating G-NN potential by learning GM structures. Bayesian optimization is terminated until the GM predicted from SSW-NN is confirmed after more than 5 Bayesian cycles.

2. Training dataset of the CeZrO G-NN potential

Table S1 | Structure information in the first principles global dataset. Listed data are the number of the structures in the global dataset, as distinguished by the chemical formula (Species), the number of atoms per cell (N_{atm}), the type of structures, being layer (N_{lay}) and bulk (N_{bul}). Total number of structures (N_{tot}) are also summarized.

Species	N_{atm}	N_{lay}	N_{bul}	N_{tot}
O1-Zr12	13	1046	0	1046
O2-Zr8	10	65	151	216
O2-Zr10	12	569	0	569
O3-Zr18	21	142	71	213
O4-Zr4	8	107	371	478
O4-Zr8	12	62	225	287
O4-Zr22	26	14	62	76
O5-Zr27	32	2	63	65
O6-Ce4	10	18	81	99
O6-Zr4	10	0	26	26
O6-Zr8	14	69	268	337
O6-Zr15	21	135	0	135
O6-Zr18	24	16	76	92
O7-Ce4	11	15	380	395
O7-Zr3-Ce1	11	9	460	469
O8-Ce4	12	68	1516	1584
O8-Zr1-Ce3	12	74	1023	1097
O8-Zr2-Ce2	12	57	902	959
O8-Zr3-Ce1	12	12	935	947
O8-Zr4	12	107	9729	9836
O8-Zr8	16	60	238	298
O8-Zr15	23	22	87	109

O10-Zr8	18	85	297	382
O10-Zr22	32	1	71	72
O11-Zr1-Ce6	18	0	20	20
O11-Zr2-Ce5	18	0	21	21
O12-Ce8	20	0	31	31
O12-Zr8	20	0	259	259
O13-Ce7	20	2	2	4
O13-Ce8	21	0	3	3
O13-Zr2-Ce5	20	1	0	1
O13-Zr3-Ce4	20	1	0	1
O13-Zr4-Ce3	20	0	1	1
O13-Zr5-Ce2	20	2	0	2
O13-Zr6-Ce1	20	1	1	2
O13-Zr7	20	24	10	34
O13-Zr7-Ce1	21	0	9	9
O14-Ce8	22	0	27	27
O14-Ce9	23	0	2	2
O14-Zr1-Ce7	22	0	14	14
O14-Zr2-Ce6	22	0	11	11
O14-Zr3-Ce5	22	0	3	3
O14-Zr4-Ce4	22	0	1	1
O14-Zr5-Ce3	22	0	4	4
O14-Zr6-Ce2	22	0	8	8
O14-Zr7-Ce1	22	0	9	9
O14-Zr8	22	0	122	122
O14-Zr8-Ce1	23	0	7	7
O15-Ce8	23	0	18	18
O15-Ce9	24	0	25	25
O15-Zr1-Ce7	23	0	27	27
O15-Zr1-Ce8	24	0	4	4
O15-Zr2-Ce6	23	0	18	18
O15-Zr2-Ce7	24	0	8	8
O15-Zr3-Ce5	23	0	29	29
O15-Zr3-Ce6	24	0	7	7
O15-Zr4-Ce4	23	16	38	54
O15-Zr4-Ce5	24	0	2	2
O15-Zr5-Ce3	23	0	57	57
O15-Zr5-Ce4	24	0	12	12
O15-Zr6-Ce2	23	1	51	52
O15-Zr6-Ce3	24	0	3	3
O15-Zr7-Ce1	23	1	129	130
O15-Zr7-Ce2	24	1	10	11
O15-Zr8-Ce1	24	1	12	13
O15-Zr9	24	1	194	195

O16-Ce8	24	25	32	57
O16-Zr1-Ce7	24	38	53	91
O16-Zr2-Ce6	24	47	55	102
O16-Zr3-Ce5	24	67	98	165
O16-Zr4-Ce4	24	29	62	91
O16-Zr5-Ce3	24	172	100	272
O16-Zr6-Ce1	23	2	87	89
O16-Zr6-Ce2	24	20	2	22
O17-Zr4-Ce6	27	1	11	12
O18-Zr12	30	232	11	243
O19-Zr2-Ce10	31	2	8	10
O22-Zr4-Ce10	36	0	5	5
O22-Zr8-Ce4	34	2	10	12
O23-Zr2-Ce10	35	0	13	13
O23-Zr3-Ce9	35	1	7	8
O23-Zr5-Ce7	35	0	8	8
O23-Zr7-Ce5	35	0	10	10
O23-Zr8-Ce4	35	0	20	20
O23-Zr9-Ce3	35	0	32	32
O23-Zr10-Ce2	35	0	29	29
O23-Zr11-Ce1	35	0	10	10
O24-Ce16	40	0	12	12
O24-Zr1-Ce11	36	3	26	29
O24-Zr2-Ce10	36	2	34	36
O24-Zr3-Ce9	36	2	29	31
O24-Zr3-Ce12	39	0	6	6
O24-Zr4-Ce8	36	0	13	13
O24-Zr6-Ce6	36	0	26	26
O24-Zr7-Ce5	36	0	10	10
O24-Zr8-Ce4	36	1	28	29
O24-Zr9-Ce3	36	0	14	14
O24-Zr10-Ce2	36	0	9	9
O24-Zr11-Ce1	36	1	26	27
O26-Zr2-Ce13	41	0	2	2
O26-Zr4-Ce12	42	0	6	6
O26-Zr14-Ce2	42	0	4	4
O28-Ce16	44	0	10	10
O28-Zr2-Ce13	43	0	1	1
O28-Zr2-Ce14	44	0	7	7
O28-Zr4-Ce12	44	0	3	3
O28-Zr9-Ce6	43	0	2	2
O28-Zr10-Ce6	44	0	1	1
O28-Zr12-Ce4	44	2	3	5
O28-Zr14-Ce1	43	0	9	9

O28-Zr14-Ce2	44	0	2	2
O28-Zr16-Ce2	46	1	4	5
O29-Zr14-Ce1	44	9	2	11
O30-Ce16	46	3	7	10
O30-Ce18	48	1	3	4
O30-Zr1-Ce15	46	0	8	8
O30-Zr2-Ce13	45	0	3	3
O30-Zr2-Ce14	46	0	29	29
O30-Zr2-Ce16	48	0	1	1
O30-Zr4-Ce12	46	0	4	4
O30-Zr5-Ce10	45	0	4	4
O30-Zr6-Ce9	45	0	3	3
O30-Zr6-Ce10	46	1	19	20
O30-Zr6-Ce12	48	0	11	11
O30-Zr8-Ce8	46	8	21	29
O30-Zr8-Ce10	48	1	0	1
O30-Zr9-Ce6	45	0	5	5
O30-Zr10-Ce5	45	1	1	2
O30-Zr10-Ce6	46	0	49	49
O30-Zr10-Ce8	48	0	6	6
O30-Zr12-Ce4	46	5	36	41
O30-Zr12-Ce6	48	0	3	3
O30-Zr13-Ce2	45	2	0	2
O30-Zr14-Ce2	46	7	128	135
O30-Zr14-Ce4	48	1	5	6
O30-Zr16-Ce2	48	2	7	9
O31-Zr6-Ce10	47	4	0	4
O31-Zr8-Ce10	49	0	9	9
O31-Zr15-Ce1	47	17	4	21
O32-Ce16	48	2	12	14
O32-Zr2-Ce14	48	31	60	91
O32-Zr4-Ce12	48	5	17	22
O32-Zr4-Ce16	52	0	3	3
O32-Zr6-Ce10	48	50	133	183
O32-Zr8-Ce8	48	9	21	30
O32-Zr10-Ce6	48	57	139	196
O32-Zr10-Ce8	50	2	15	17
O32-Zr11-Ce5	48	3	0	3
O32-Zr12-Ce2	46	12	141	153
O32-Zr12-Ce4	48	4	2	6
O32-Zr14-Ce2	48	9	2	11
O33-Zr6-Ce14	53	2	12	14
O33-Zr12-Ce6	51	1	9	10
O34-Zr8-Ce12	54	2	6	8

O36-Zr12-Ce8	56	2	11	13
O37-Zr14-Ce6	57	1	6	7
O38-Zr4-Ce20	62	0	5	5
O38-Zr10-Ce12	60	0	7	7
O39-Zr6-Ce18	63	0	6	6
O40-Zr8-Ce16	64	0	11	11
O44-Zr16-Ce8	68	3	4	7
O46-Zr4-Ce20	70	1	5	6
O46-Zr6-Ce18	70	0	5	5
O46-Zr10-Ce14	70	0	1	1
O46-Zr14-Ce10	70	0	3	3
O46-Zr16-Ce8	70	0	7	7
O46-Zr18-Ce6	70	1	9	10
O46-Zr20-Ce4	70	4	17	21
O46-Zr22-Ce2	70	0	3	3
O48-Ce32	80	0	1	1
O48-Zr2-Ce22	72	1	5	6
O48-Zr4-Ce20	72	1	7	8
O48-Zr6-Ce18	72	0	8	8
O48-Zr6-Ce24	78	0	112	112
O48-Zr12-Ce12	72	1	5	6
O48-Zr14-Ce10	72	1	3	4
O48-Zr15-Ce12	75	0	6	6
O48-Zr16-Ce8	72	1	8	9
O48-Zr18-Ce6	72	1	2	3
O48-Zr20-Ce4	72	1	2	3
O48-Zr22-Ce2	72	3	6	9
O51-Zr12-Ce18	81	0	8	8
O52-Zr8-Ce24	84	0	1	1
O56-Zr2-Ce28	86	0	1	1
O56-Zr4-Ce26	86	1	0	1
O56-Zr4-Ce28	88	0	2	2
O56-Zr18-Ce12	86	1	0	1
O56-Zr28-Ce2	86	2	6	8
O58-Zr28-Ce2	88	4	6	10
O60-Zr2-Ce30	92	0	1	1
O60-Zr4-Ce28	92	0	1	1
O60-Zr10-Ce20	90	0	1	1
O60-Zr12-Ce20	92	0	2	2
O60-Zr12-Ce24	96	0	9	9
O60-Zr18-Ce12	90	0	2	2
O60-Zr20-Ce12	92	1	8	9
O60-Zr24-Ce8	92	0	3	3
O60-Zr26-Ce4	90	1	0	1

O60-Zr28-Ce4	92	6	21	27
O62-Zr12-Ce20	94	0	1	1
O62-Zr16-Ce20	98	0	1	1
O62-Zr30-Ce2	94	2	7	9
O63-Zr26-Ce6	95	3	4	7
O63-Zr28-Ce4	95	6	8	14
O63-Zr30-Ce2	95	11	15	26
O64-Ce32	96	8	4	12
O64-Zr1-Ce31	96	6	0	6
O64-Zr4-Ce28	96	4	6	10
O64-Zr8-Ce32	104	0	1	1
O64-Zr12-Ce20	96	10	32	42
O64-Zr20-Ce12	96	4	34	38
O64-Zr22-Ce10	96	2	0	2
O64-Zr24-Ce4	92	10	19	29
O64-Zr26-Ce6	96	3	8	11
O64-Zr28-Ce4	96	17	18	35
O64-Zr30-Ce2	96	1	5	6
O66-Zr12-Ce28	106	0	15	15
O66-Zr24-Ce12	102	0	3	3
O68-Zr16-Ce24	108	0	5	5
O72-Zr24-Ce16	112	1	5	6
O74-Zr28-Ce12	114	0	4	4
O76-Zr20-Ce24	120	0	8	8
O78-Zr12-Ce36	126	0	2	2
O80-Zr16-Ce32	128	0	1	1
O96-Zr12-Ce48	156	0	8	8
O96-Zr30-Ce24	150	0	1	1
O102-Zr24-Ce36	162	0	3	3
O126-Zr52-Ce12	190	0	7	7
O126-Zr56-Ce8	190	1	2	3
O126-Zr60-Ce4	190	0	9	9
O128-Ce64	192	1	2	3
O128-Zr2-Ce62	192	0	1	1
O128-Zr52-Ce12	192	1	3	4
O128-Zr56-Ce8	192	0	4	4
O128-Zr60-Ce4	192	1	0	1
total	--	3838	20714	24552

Table S2| Training Error distribution on slab and bulk dataset

	RMSE Energy (meV)	RMSE force (eV/ Å)
Slab	4.623	0.153
Bulk	5.659	0.137

3. Benchmark of G-NN potential against DFT calculations

Table S3 | Benchmark of NN calculations for CZO systems as compared with DFT results. Listed data includes the compositions, structure, DFT energy, NN energy and energy differences between DFT energy and NN energy (E_{diff}, meV/atom)

No.	Species	N_{atom}	EDFT/eV	E_{nn}/eV	$\Delta(E_{nn}-E_{DFT})$/(meV/atom)
1	Ce12Zr8O34(GM)	54	-483.262	-483.273	-0.185
2	Ce4Zr4O14(GM)	22	-199.684	-199.580	4.545
3	Ce16Zr16O60	92	-820.778	-821.150	-4.043
4	Ce16Zr16O61	93	-826.499	-826.749	-2.690
5	Ce16Zr16O64	96	-841.865	-841.789	0.790
6	Ce4Zr4O16(GM)	24	-211.062	-210.960	4.218
7	Ce6Zr2O15(GM)	23	-197.038	-197.044	-0.198
8	Ce6Zr2O15(str1)	23	-196.985	-196.896	3.870
9	Ce6Zr2O15(str2)	23	-196.888	-196.842	2.015
10	Ce24Zr6O48(GM)	78	-676.502	-676.816	-4.032
11	Ce24Zr6O48(str1)	78	-676.417	-676.807	-4.992
	RMS				2.871

4. Benchmark of thermodynamics among different computational methods

BEEF-vdW: Taking the O adsorption in R-CZ50 as example, BEEF-vdW functional, PBE functional and PBE-D3 functional give the G_{ad}^{θ} at room temperature -0.29, 0.40 and 0.66 eV/atom. This suggests R-CZ50 is resistive to oxidation at room temperature under BEEF functional, which is inconsistent with the experimental observation that R-CZ50 can be slowly oxidized at room temperature[1].

PBE-D3: To better compare PBE and PBE-D3 we have plotted the thermodynamics diagrams as shown in the Figure S1. The results show that the thermodynamics diagrams calculated using PBE align better with the experimental observation, i.e., the oxygen storage capacity of R-CZ50 at 773 K is 89%[2], whereas the one obtained using PBE-D3 is too high (100%). Overall, we found PBE functional is generally good to describe the CZO system, which provides the most reasonable picture to compare with experiment.

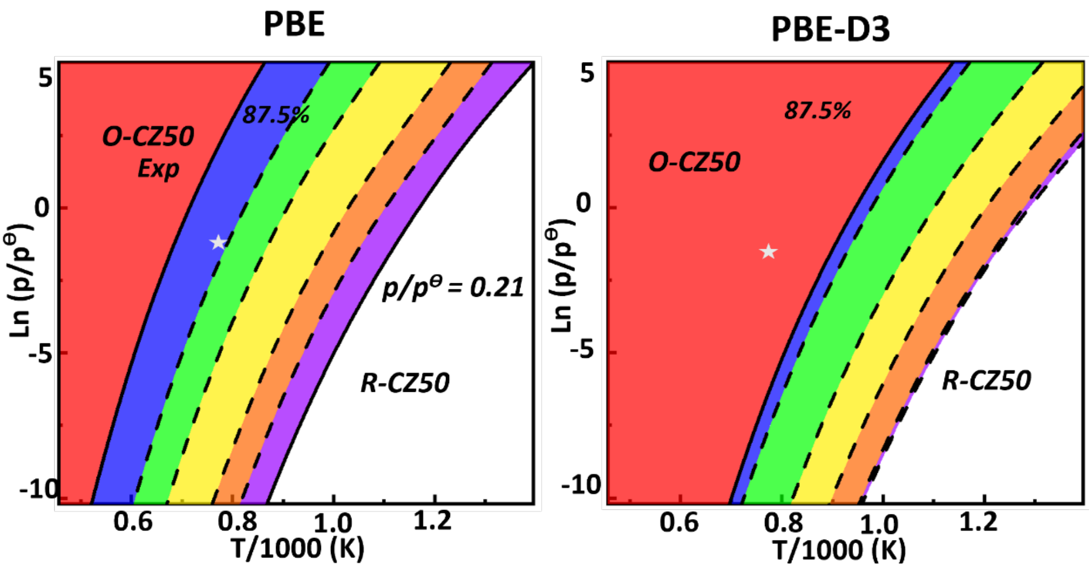

Figure S1 | Thermodynamics diagrams of R-CZ50 (PBE, left panel) and R-CZ50 (PBE-D3, right panel) under different conditions. The white star indicates the experimental results (773k and 1atm).

Table S4 | The benchmark of barrier energy (E_a, eV) using PBE functional with D3 dispersion correction (PBE-D3).

	R-CZ50 w/o. d3	R-CZ50 w. d3
E_a (TS1)	0.32	0.32
E_a (TS2)	0.70	0.67
E_a (TS3)	0.02	0.013
E_a (TS4)	0.50	0.47
	R-CZ60 w/o. d3	R-CZ60 w. d3
E_a (TS5)	0.26	0.28
E_a (TS6)	0.20	0.18
E_a (TS7)	0.14	0.13
E_a (TS8)	0.38	0.42

5. The RDF of the Ce-Ce, Zr-Zr and Zr-Ce of CZ50 and R-CZ50

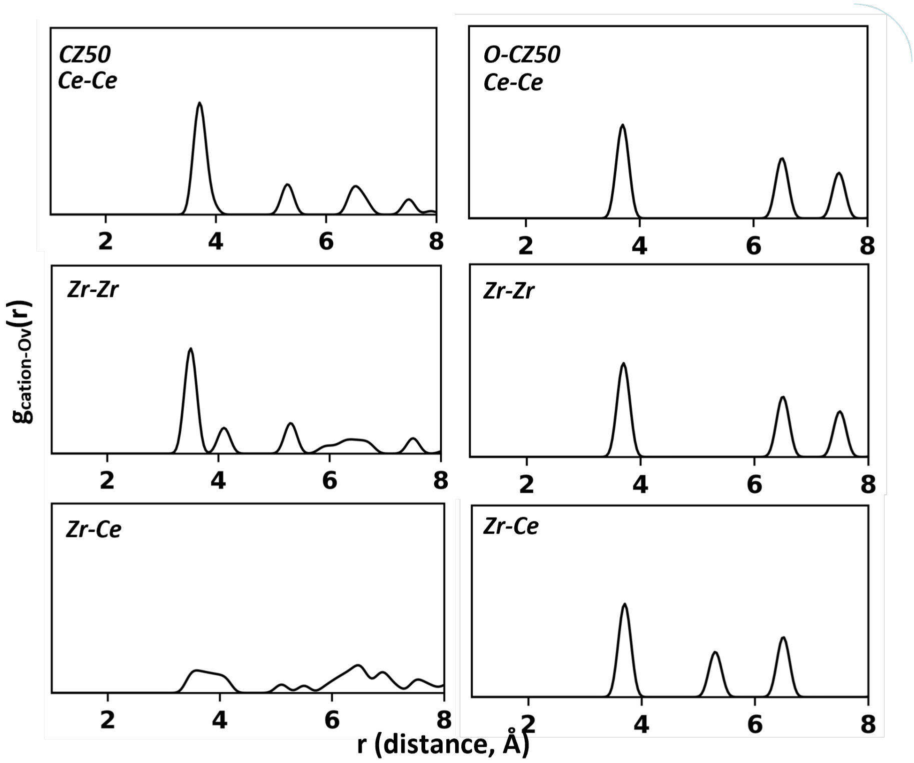

Figure S2 | Radial distribution function g(r) of the Ce-Ce, Zr-Zr and Zr-Ce of CZ50 and R-CZ50.

6. The atomic structures and simulated XRD of R-CZ66 and R-CZ75

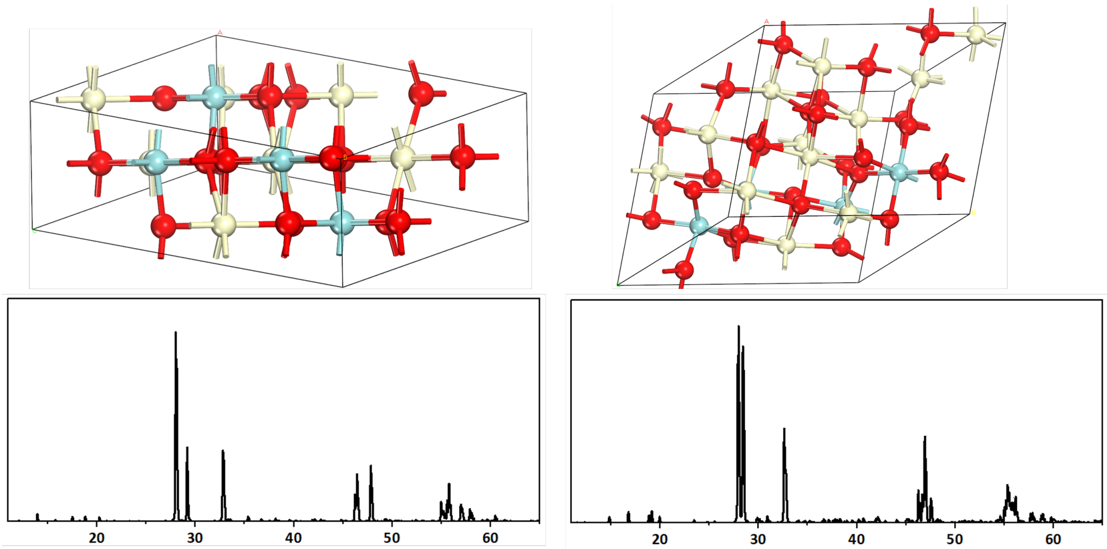

Figure S3 | The atomic structures and simulated x-ray diffraction patterns of GM of R-CZ66 and R-CZ75.

7. Thermodynamics diagrams of R-CZ80

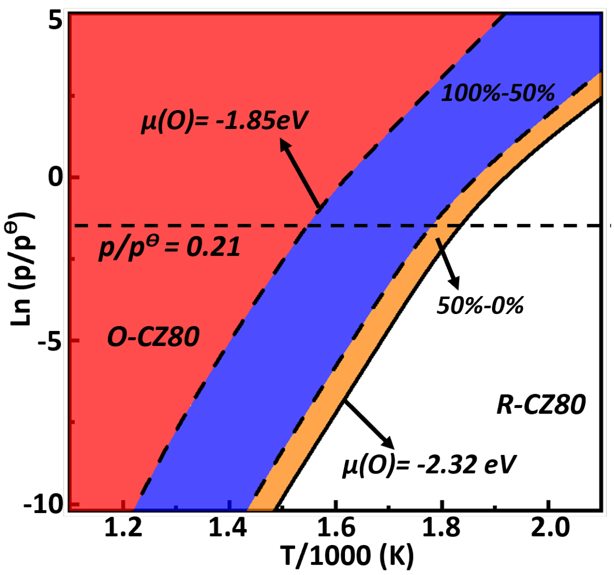

Figure S4 | Thermodynamics diagrams of R-CZ80. Cationic position is kept fixed in constructing the thermodynamics diagrams.

8. The experimental and simulated XRD patterns for Ce: Zr=1:1 sample.

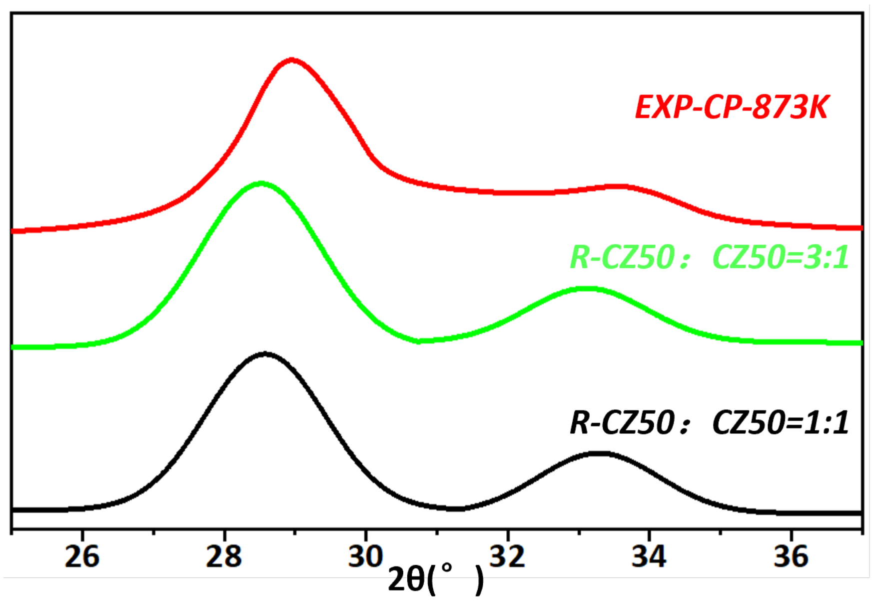

Figure S5| The experimental (Exp) and theoretical XRD patterns for Ce: Zr=1:1 sample. The co-precipitation (CP) method: red line; The theoretical XRD are simulated with component of R-CZ50: CZ50 = 3:1 (green line) and 1:1 (black line).

9. The RDF of Ce-O_v, Zr-O_v and O_v-O_v in R-CZ80

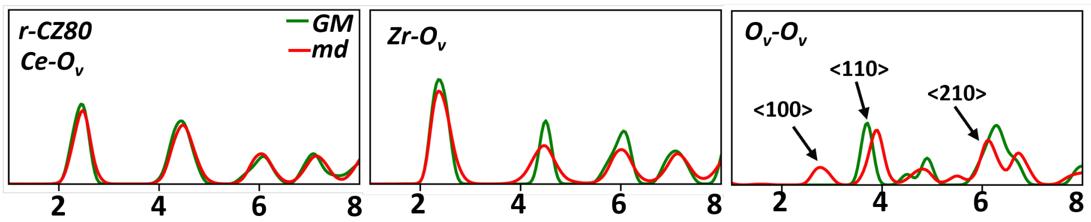

Figure S6 | Radial distribution function g(r) of the cation (Zr, Ce)−O_v and O_v-O_v pairs at 2400 K from the averaged snapshots of MD simulations (red lines) to compare with their GM structures (green lines).

10. The snapshots of the O_{2c} diffusion pathway

We likewise note the presence of interstitial oxygen O_{2c} in the system. As shown in Fig. S7, the two O_v, being 3.80 Å apart, locate along the <110> direction in the initial state, where the O_{2c}(2Zr) can diffuse to O_v(2Ce2Zr) along the <010> direction through a very low energy barrier of 0.07 eV and leads finally to the formation of two Ov (1Ce3Zr) along the <100> direction, followed by the diffusion of O from <100> to <110>

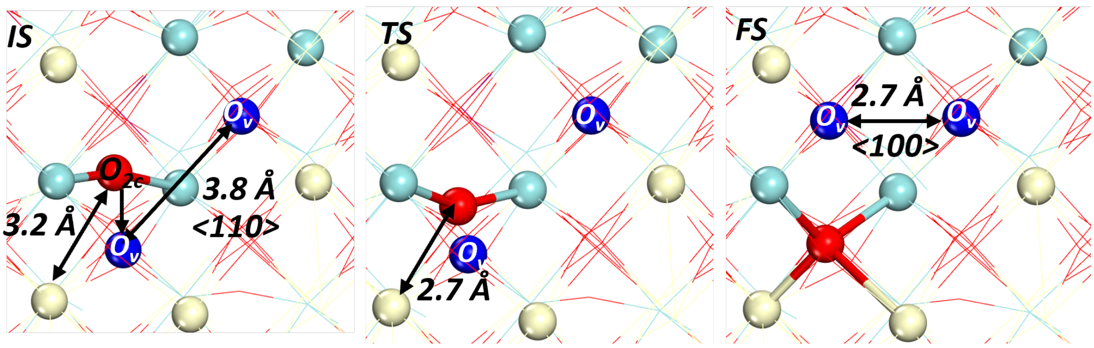

Figure S7| The snapshots of the O_{2c}(2Zr) diffusion pathway along <010> direction in R-CZ60. Blue ball: O_v; red ball: O; cyan ball: Zr; yellow ball: Ce.

direction in Fig. 4c. Overall, the presence of this interstitial oxygen provides a diffusion pathway for the O_v from <110> to <100>.

11. The surface O_v pattern of 25% O filled R-CZ50 (111) and 33.3% O filled R-CZ60 (201)

The procedure to identify the bulk and surface O_v concentration

Taking R-CZ50 as an example:

Firstly, we added different O into R-CZ50 conventional cell ($Ce_{16}Zr_{16}O_{56}$) with 8 O_v; secondly, for each O_v concentration, we start from the same structure and run 5 pathways in parallel using SSW-NN for more than 25000 steps totally to search for its global minimum (GM). Then, we cleave the four layers slab model of (111) surface based on the GM and get the Ov sites on the surface. Finally, the energy of $E(CO_2)$-$E(CO)$ is used to estimate whether the O can be added on surface to fill the O_v.

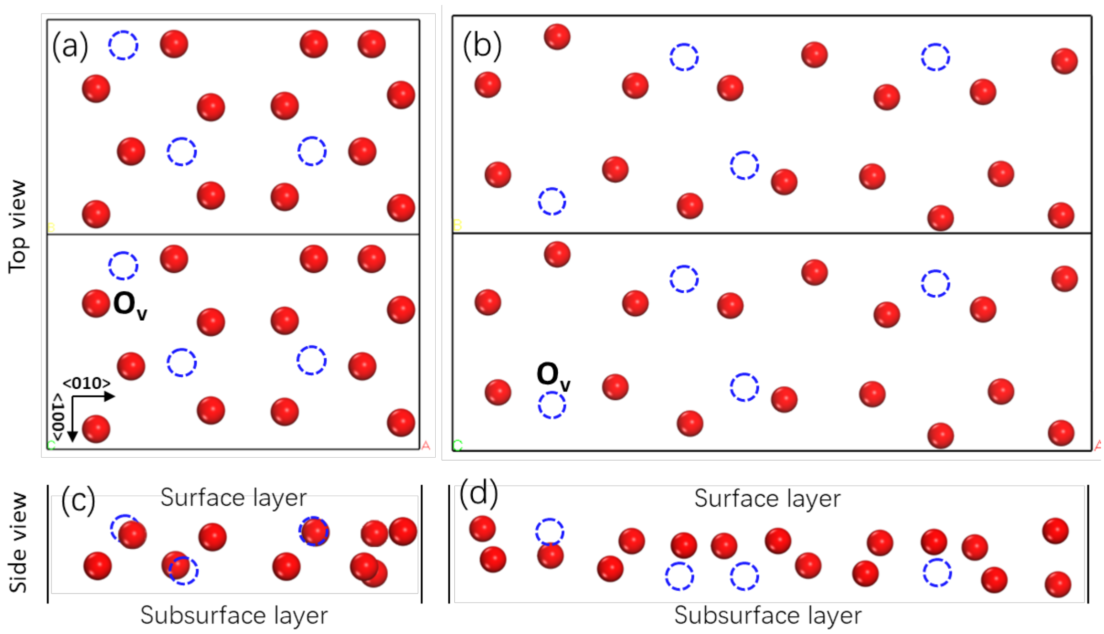

Figure S8 | The surface and subsurface O_v pattern of 25% O filled R-CZ50 (111) (a, c) and 33.3% O filled R-CZ60 (201) (b, d). Blue circle: O_v; red ball: lattice O.

12. The snapshots of CO oxidation at (201) surface of 100% O filled R-CZ60

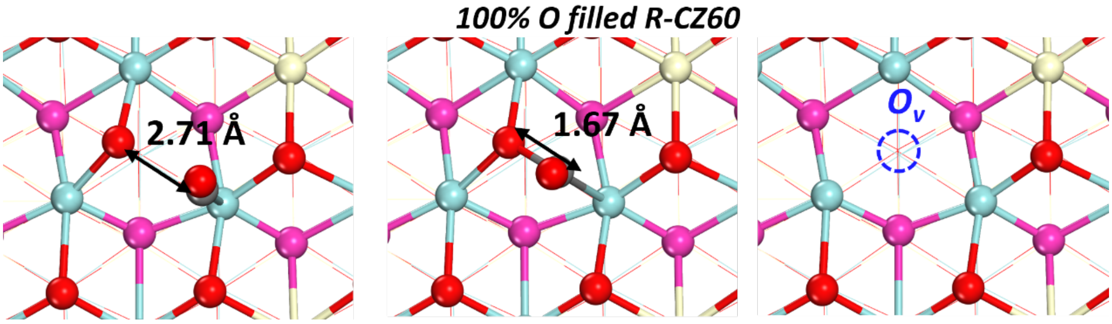

Figure S9 | The snapshots of CO oxidation at (201) surface of 100% O filled R-CZ60.

13. The snapshots of CO oxidation at (111) surface of 25% O filled R-CZ50 and (201) surface of 33.3% O filled R-CZ60

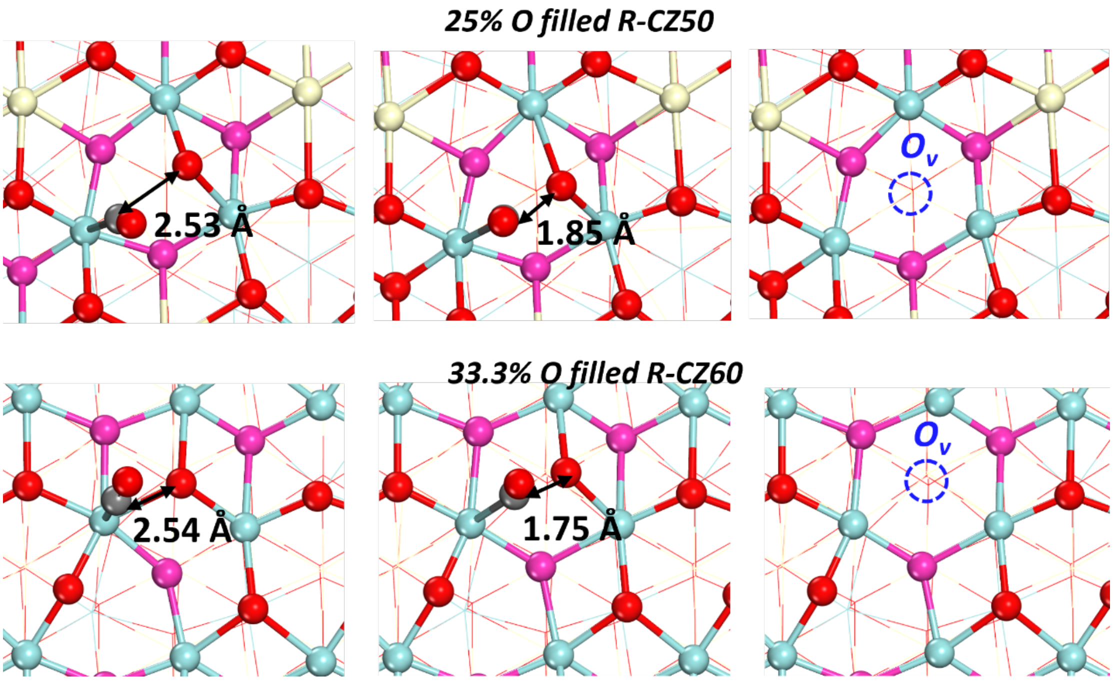

Figure S10| The snapshots of CO oxidation at (111) surface of 25% O filled R-CZ50 and (201) surface of 33.3% O filled R-CZ60.

14. The slab model of 25% O filled R-CZ50 and 33.3% O filled R-CZ60

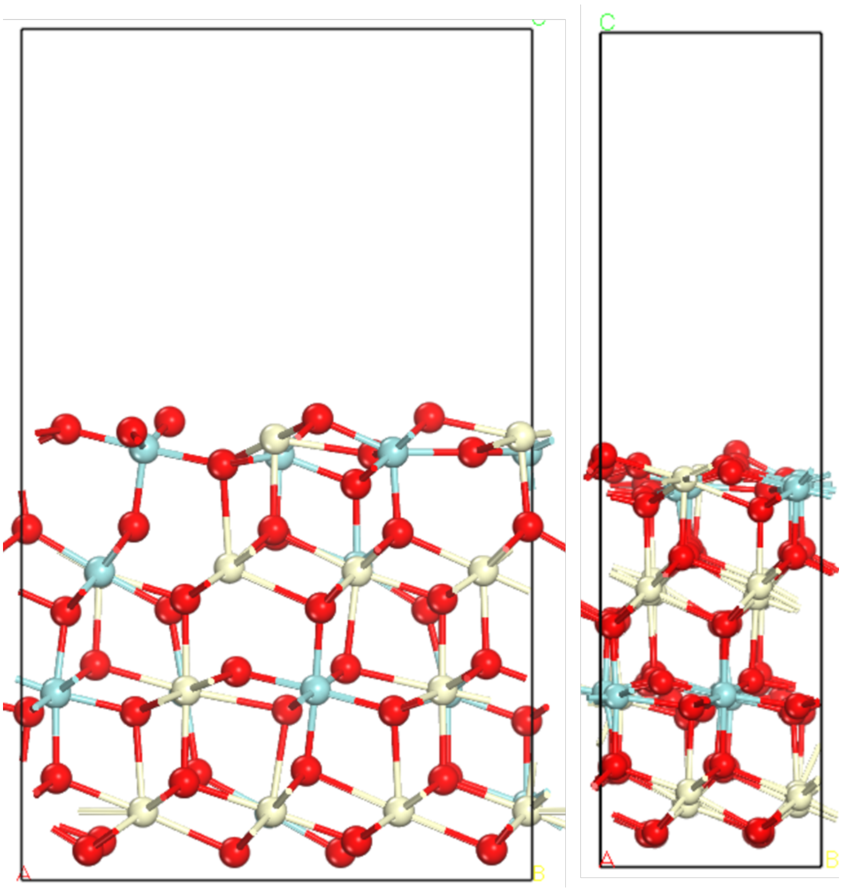

Figure S11| The slab model of 25% O filled R-CZ50 and 33.3% O filled R-CZ60.

15. Optimized XYZ positions for R-CZ60, *R*-CZ80 and CZ50

!BIOSYM archive 3

PBC=ON

Materials Studio Generated CAR File

!DATE Thu Jan 18 15:46:58 2024

PBC 13.3164 6.7428 10.3049 77.4640 70.9208 99.7451 (P1)

Zr	7.027112774	7.244955919	5.648760043	CORE 1	Zr	Zr	0.000
Zr	13.860408834	3.354959891	7.261960476	CORE 2	Zr	Zr	0.000
Zr	2.500859092	4.134356451	0.076489331	CORE 3	Zr	Zr	0.000
Zr	13.682307731	7.216610617	5.646865821	CORE 4	Zr	Zr	0.000
O	10.702835229	6.718924499	8.842940529	CORE 5	O	O	0.000
O	3.306301927	4.219260224	4.460309401	CORE 6	O	O	0.000
O	11.235138505	4.722001920	0.726655178	CORE 7	O	O	0.000
O	14.272184309	5.181631162	6.054017538	CORE 8	O	O	0.000
O	8.931623815	1.426478440	3.855778277	CORE 9	O	O	0.000
O	8.676239407	5.351849640	2.115665075	CORE 10	O	O	0.000
O	10.409311405	4.283435486	4.447347478	CORE 11	O	O	0.000
Zr	9.293431683	0.780120682	1.899156283	CORE 12	Zr	Zr	0.000
Zr	1.311946021	4.406744554	4.023297178	CORE 13	Zr	Zr	0.000
Zr	1.525981939	7.044916762	1.679475069	CORE 14	Zr	Zr	0.000
Zr	9.166041320	4.534204647	0.267185055	CORE 15	Zr	Zr	0.000
O	9.494706991	2.649611187	1.100635860	CORE 16	O	O	0.000
O	0.716260211	6.461798470	3.687564623	CORE 17	O	O	0.000
O	4.521465531	4.659091692	0.462394450	CORE 18	O	O	0.000
O	5.987152482	3.632122012	3.051407158	CORE 19	O	O	0.000
O	6.230717392	6.429904038	7.437912042	CORE 20	O	O	0.000
O	5.103119840	6.666503110	4.871439732	CORE 21	O	O	0.000
O	3.832025003	6.566015544	8.852193100	CORE 22	O	O	0.000
O	11.351935977	1.066968723	2.589784305	CORE 23	O	O	0.000
O	5.162550890	9.019127479	9.114405113	CORE 24	O	O	0.000
Ce	11.556957876	2.272747998	4.729894087	CORE 25	Ce	Ce	0.000
Ce	2.658504303	8.760368414	8.464166978	CORE 26	Ce	Ce	0.000
Ce	12.307622047	2.518802320	0.986758794	CORE 27	Ce	Ce	0.000
Ce	4.585167500	5.599290186	2.805154868	CORE 28	Ce	Ce	0.000
Ce	11.514765239	5.769817428	2.903684607	CORE 29	Ce	Ce	0.000
Ce	3.588436381	5.534528926	6.598664371	CORE 30	Ce	Ce	0.000
Ce	10.224547687	5.555946709	6.566648069	CORE 31	Ce	Ce	0.000
Ce	9.471403506	8.893442601	8.542811083	CORE 32	Ce	Ce	0.000
Ce	4.960847823	2.251293550	4.771307893	CORE 33	Ce	Ce	0.000
O	14.239906926	2.599813729	5.218904065	CORE 34	O	O	0.000
O	7.247501513	0.509076759	1.528732987	CORE 35	O	O	0.000
O	0.654102453	0.579799257	1.264554364	CORE 36	O	O	0.000
O	9.167005622	4.150053447	8.237440461	CORE 37	O	O	0.000

O	4.436004795	0.998659362	2.648125569 CORE 38	O	O	0.000
O	7.204065459	2.478220179	5.777122557 CORE 39	O	O	0.000
O	13.014754472	2.829951263	9.186810914 CORE 40	O	O	0.000
O	3.084978575	2.232330267	0.707231758 CORE 41	O	O	0.000
O	13.229438858	7.922870749	7.575903935 CORE 42	O	O	0.000
O	4.774191467	3.568377966	6.839051816 CORE 43	O	O	0.000
O	11.671565363	6.832278715	5.200104218 CORE 44	O	O	0.000
O	11.873181802	3.599484924	6.828553997 CORE 45	O	O	0.000
Ce	6.938789397	4.087945958	7.458429561 CORE 46	Ce	Ce	0.000
Ce	8.229661550	3.749374402	3.851869595 CORE 47	Ce	Ce	0.000
Ce	5.682738851	2.487690553	0.997109925 CORE 48	Ce	Ce	0.000
O	15.537876434	4.061132316	8.224650745 CORE 49	O	O	0.000
O	2.151050404	4.952363431	2.086427953 CORE 50	O	O	0.000
O	2.364180784	7.632441777	6.167445242 CORE 51	O	O	0.000
O	12.938025615	3.699282804	3.054556152 CORE 52	O	O	0.000
O	7.973680875	5.348268860	5.532497101 CORE 53	O	O	0.000
O	8.951232137	7.790312859	6.464823047 CORE 54	O	O	0.000

end

end

```
!BIOSYM archive 3
PBC=ON
Materials Studio Generated CAR File
!DATE Thu Jan 18 15:51:20 2024
PBC   12.4694   11.8158    9.5881  105.3370   72.4749   85.9346 (P1)
O        9.069442215    9.404197913    3.089465754 CORE 1      O      O    0.000
O       14.928347281    2.503668666    8.582426513 CORE 2      O      O    0.000
O        2.470110720    2.895350407    1.153729140 CORE 3      O      O    0.000
O        3.739534689    1.880636704    5.717893012 CORE 4      O      O    0.000
O        8.713870784    7.820332332    6.395487032 CORE 5      O      O    0.000
O        2.969505878    7.842366740    6.740611540 CORE 6      O      O    0.000
O        5.607153724    0.898709870    3.835713172 CORE 7      O      O    0.000
O        9.078857584    5.742594471    0.928314341 CORE 8      O      O    0.000
O       12.303090017    9.839773986    4.062500716 CORE 9      O      O    0.000
O        7.459418442    3.577069394    4.114346011 CORE 10     O      O    0.000
O        2.365664731    0.464536576    2.867338449 CORE 11     O      O    0.000
O        5.953615973    2.482671663    0.530345891 CORE 12     O      O    0.000
O        7.108687273   11.270073173    1.437070032 CORE 13     O      O    0.000
O        3.320878813    9.421432879    3.440049406 CORE 14     O      O    0.000
O        2.355369281    5.723091956    0.578628272 CORE 15     O      O    0.000
O       13.796843855   -1.278714166    6.025238286 CORE 16     O      O    0.000
O        8.569064534    0.408798662    2.765996256 CORE 17     O      O    0.000
O        3.989076125   -1.265515211    7.022024711 CORE 18     O      O    0.000
O        4.796919660    3.560113933    3.117008964 CORE 19     O      O    0.000
O        6.403547985    1.892401715    6.715387178 CORE 20     O      O    0.000
O        8.830888324    4.988590374    6.962190426 CORE 21     O      O    0.000
O       13.574354937    8.821281244    8.625951251 CORE 22     O      O    0.000
O        8.729968950    2.564607318    8.683093111 CORE 23     O      O    0.000
O       11.349255974    0.879402450    3.485316510 CORE 24     O      O    0.000
O        8.735320022    2.953414977    1.257129222 CORE 25     O      O    0.000
O        3.628848189    6.428025074    4.341605252 CORE 26     O      O    0.000
O       12.319957321    4.576728165    6.347151037 CORE 27     O      O    0.000
O       13.718490631    3.642225330    3.916845580 CORE 28     O      O    0.000
O        7.211462501    6.725579276    2.813011818 CORE 29     O      O    0.000
O       10.933224293    8.417476104    1.205800583 CORE 30     O      O    0.000
O        9.951790418    1.815170152    5.920438352 CORE 31     O      O    0.000
O        6.103705681    9.893410516    4.158258145 CORE 32     O      O    0.000
O        9.871230279    6.738630247    3.809886802 CORE 33     O      O    0.000
O        4.929512394    5.975919105    8.398939938 CORE 34     O      O    0.000
O       12.511627274   -0.201989566    0.900474503 CORE 35     O      O    0.000
O       13.421556219    6.665027079    3.009859243 CORE 36     O      O    0.000
O        4.722872026    8.484269498    1.007457199 CORE 37     O      O    0.000
O       15.100620768    5.050626052    7.066082988 CORE 38     O      O    0.000
O       11.700799411    2.459821509    0.185644510 CORE 39     O      O    0.000
```

O	8.269208815	8.408775400	0.210780606	CORE	40	O	O	0.000
O	11.039775126	3.874280893	2.585878077	CORE	41	O	O	0.000
O	5.932818342	7.349921024	5.671714911	CORE	42	O	O	0.000
O	7.568764084	-0.973040907	5.492099523	CORE	43	O	O	0.000
O	12.631652499	1.578605971	7.248002365	CORE	44	O	O	0.000
O	4.432640129	11.502674191	0.106051480	CORE	45	O	O	0.000
O	10.244988777	-1.203834069	6.827935241	CORE	46	O	O	0.000
O	12.201702447	7.404240583	5.771097076	CORE	47	O	O	0.000
O	5.593331651	4.557606349	6.000461976	CORE	48	O	O	0.000
Ce	6.824254586	4.345544404	1.849574268	CORE	49	Ce	Ce	0.000
Ce	5.189591682	7.938283773	3.290926925	CORE	50	Ce	Ce	0.000
Ce	7.827770190	0.994353678	0.387647361	CORE	51	Ce	Ce	0.000
Ce	6.900856611	4.038087630	8.066692543	CORE	52	Ce	Ce	0.000
Ce	2.880932982	10.300644108	1.289167056	CORE	53	Ce	Ce	0.000
Ce	8.406472613	0.605331918	7.103740918	CORE	54	Ce	Ce	0.000
Ce	14.187733307	3.095487290	6.199403174	CORE	55	Ce	Ce	0.000
Ce	13.183259297	6.441856918	7.664577402	CORE	56	Ce	Ce	0.000
Ce	3.349500458	-0.500566783	4.756708384	CORE	57	Ce	Ce	0.000
Ce	7.849518811	5.955148518	5.077296137	CORE	58	Ce	Ce	0.000
Ce	11.318827712	10.802083547	2.170887472	CORE	59	Ce	Ce	0.000
Ce	4.377683533	1.111843491	7.982439520	CORE	60	Ce	Ce	0.000
Ce	11.876298630	5.452691889	4.197043578	CORE	61	Ce	Ce	0.000
Ce	10.372784973	8.888235034	5.167480259	CORE	62	Ce	Ce	0.000
Ce	13.005370888	1.948534697	2.258099254	CORE	63	Ce	Ce	0.000
Ce	10.659582980	3.517982864	7.579852274	CORE	64	Ce	Ce	0.000
Ce	14.136044085	8.353041673	4.669052341	CORE	65	Ce	Ce	0.000
Ce	4.297517700	1.421305652	1.764566048	CORE	66	Ce	Ce	0.000
Ce	12.956510130	7.206596269	0.727166340	CORE	67	Ce	Ce	0.000
Ce	6.850051078	9.308167752	6.542477435	CORE	68	Ce	Ce	0.000
Ce	9.486831814	2.368250566	3.637590736	CORE	69	Ce	Ce	0.000
Ce	2.795506110	4.849699878	2.731586598	CORE	70	Ce	Ce	0.000
Ce	9.152773826	6.950797104	8.546097736	CORE	71	Ce	Ce	0.000
Ce	11.792121632	0.001883563	5.638853366	CORE	72	Ce	Ce	0.000
Zr	4.283557018	6.201501776	6.372314698	CORE	73	Zr	Zr	0.000
Zr	6.916744136	-0.743436166	3.462138121	CORE	74	Zr	Zr	0.000
Zr	10.387963836	4.100119971	0.553229635	CORE	75	Zr	Zr	0.000
Zr	9.072940940	7.573327242	2.011064741	CORE	76	Zr	Zr	0.000
Zr	14.597758607	-2.115896989	7.824152606	CORE	77	Zr	Zr	0.000
Zr	5.601027451	2.727899966	4.917877132	CORE	78	Zr	Zr	0.000

end

end

```
!BIOSYM archive 3
PBC=ON
Materials Studio Generated CAR File
!DATE Thu Jan 18 16:03:33 2024
PBC    5.3600    5.4142    10.6246    94.0457    89.9997    90.0001 (P1)
O     0.222712204    3.520524684    3.656285128 CORE 1     O     O    0.000
O     0.574316236    2.583362053    6.227156539 CORE 2     O     O    0.000
O     0.388868956   -0.194395146    8.805942831 CORE 3     O     O    0.000
O     3.288483705    0.392342143    1.201277268 CORE 4     O     O    0.000
O     0.975266197    0.813600191    3.656042601 CORE 5     O     O    0.000
O     0.809200699    2.512611767    8.805843614 CORE 6     O     O    0.000
O     3.303290122    2.743530557    6.614617581 CORE 7     O     O    0.000
O     3.655499209    1.805391446    9.186320385 CORE 8     O     O    0.000
Zr    2.146310386    1.318396305    5.255551560 CORE 9     Zr    Zr   0.000
Ce    1.918299182    4.422216758    2.499457416 CORE 10    Ce    Ce   0.000
Zr    4.826375598    1.301742175    7.586322650 CORE 11    Zr    Zr   0.000
Ce    4.639096463    1.715114371    2.499493170 CORE 12    Ce    Ce   0.000
O     0.608583450    2.977456149    1.043014199 CORE 13    O     O    0.000
O     0.623308703   -0.123808458    6.227258878 CORE 14    O     O    0.000
O     3.489430359    0.108068348    4.036372463 CORE 15    O     O    0.000
O     3.254325621    0.036482434    6.614448821 CORE 16    O     O    0.000
O     3.268921331    3.099439475    1.201195431 CORE 17    O     O    0.000
O     0.588834443    0.270369898    1.043047874 CORE 18    O     O    0.000
O     2.902598107    4.512634216    9.186121919 CORE 19    O     O    0.000
O     3.068470812    2.815152440    4.036302037 CORE 20    O     O    0.000
Zr    1.731198519    4.008841404    7.586381875 CORE 21    Zr    Zr   0.000
Ce    4.598359468    3.612035406   10.342785493 CORE 22    Ce    Ce   0.000
Zr    4.411148203    4.025441726    5.255531770 CORE 23    Zr    Zr   0.000
Ce    1.959140155    0.904932873   10.342721631 CORE 24    Ce    Ce   0.000
end
end
```

16. Reference

(1) Sasaki, T.; Ukyo, Y.; Suda, A.; Sugiura, M.; Kuroda, K.; Arai, S.; Saka, H. Oxygen Absorption Behavior of Ce₂Zr₂O_{7+x} and Formation of Ce₂Zr₂O_{7.5}. *J. Ceram. Soc. Jpn.* **2003**, *111*, 382-385

(2) Sugiura, M. Oxygen Storage Materials for Automotive Catalysts: Ceria-Zirconia Solid Solutions. *Catal. Surv. Asia* **2003**, *7*, 77-87